RSC Advances

RSC Publishing

COMMUNICATION

View Article Online
View Journal | View Issue

Cite this: *RSC Advances*, 2013, **3**, 5357

Received 22nd November 2012,
Accepted 25th February 2013

DOI: 10.1039/c3ra22998j

www.rsc.org/advances

Phase segregation in Mn-doped In_2O_3: *in situ* high-pressure high-temperature synchrotron studies in multi-anvil assemblies†

Maged F. Bekheet,*[a] Marcus R. Schwarz,[b] Mathis M. Müller,[a] Stefan Lauterbach,[a] Hans-Joachim Kleebe,[a] Ralf Riedel[a] and Aleksander Gurlo[a]

Manganese-doped bixbyite-type c-In_2O_3 decomposes into corundum-type rh-In_2O_3 and cubic MnO at 8 GPa and 950 °C.

Indium oxide (In_2O_3)—a transparent semiconductor with intrinsic n-type character—serves as a base material for diverse applications including touch displays and photovoltaics,[1] thermoelectrics,[2] and gas sensors.[3] A great deal of time and effort has been invested worldwide in synthesizing, characterizing and modeling indium oxides. A typical approach to achieve certain functional properties is to stabilize a preferred polymorph and/or control its defect chemistry.[1–3] Synthesis under high-pressure conditions generally allows for stabilizing solid state materials with unusual valence states and coordination numbers that are not accessible by other means. In the case of In_2O_3-based materials, the combination of *both* approaches, *i.e.* subjecting doped and ternary indium oxides to high-pressure appears very attractive. An example is the high-pressure-assisted synthesis of indium-based perovskites ($InMnO_3$, $InFe_{0.5}Mn_{0.5}O_3$ and $In_{0.7}Fe_{0.5}Mn_{0.5}O_{2.55}$) representing a new class of near-room temperature multiferroics.[4]

The goal of the present work is to study the effect of doping on the pressure-induced phase transitions in In_2O_3. Manganese-doping was chosen for the present study because the stable ambient pressure phases of the pure oxides (hereafter denoted as c-In_2O_3 and c-Mn_2O_3) both have bixbyite-type (space group *Ia*-3, No. 206) structure but are crystallized in different structures at higher pressures and temperatures, as displayed in Fig. 1.

With increasing pressure/temperature, c-In_2O_3 transforms into a Rh_2O_3-II-type (o′-In_2O_3, *Pbcn*, No. 60) and then to a α-Gd_2S_3-type (o″-In_2O_3, *Pnma*, No. 62) structure,[6,7] while c-Mn_2O_3 crystallizes in corundum-($R\bar{3}c$, No. 167), A-site ordered perovskite ($P\bar{1}$, No. 2) and post-perovskite (*Cmcm*, No. 63) structures.[8,9] Manganese-doped In_2O_3 may thus show a different transformation sequence, either crystallizing into yet another high pressure structure or decomposing into binary oxides.

In previous investigations laser-heated diamond-anvil cells (DACs) were employed to compress and heat c-In_2O_3 specimens.[6–7,10–12] However, temperatures below 1000 °C, where several phase transitions in In_2O_3 are expected, are very difficult to control with this technique. Externally heated DACs may be used, but would also produce very limited amounts of a high-pressure polymorph that can be recovered to ambient conditions. A synthesis method providing both *in situ* control and macroscopic quantities of the target material, suitable for physico-chemical characterization after quenching from high pressure and temperature is available in the form of large volume (multi-anvil) presses at synchrotron facilities.[13] For the present study, the phase development in Mn-doped c-In_2O_3 was followed *in situ* by energy-dispersive X-ray diffractometry at the two stage 6–8 MAX200X multi-anvil high pressure diffractometer of the GFZ Potsdam (beamline W2, HASYLAB/DESY, Hamburg, Germany).

New high-pressure/high-temperature multi-anvil assemblies for synchrotron studies developed at the Freiberg High Pressure

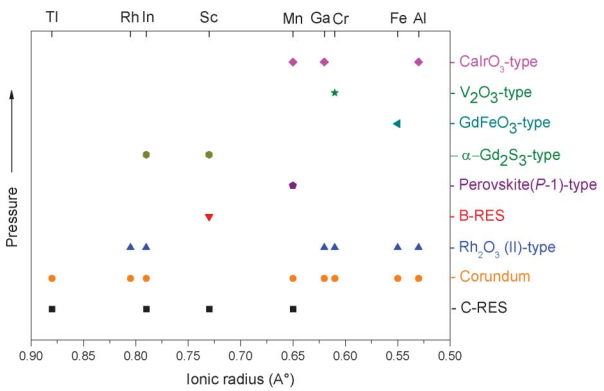

Fig. 1 Overview of ambient and high pressure crystal structures of M_2O_3 oxides with respect to the dependence on the cation radii. Corundum-type ($R\bar{3}c$, No. 167, rh-In_2O_3 hereafter) is metastable at all pressures.[5]

[a]*Fachbereich Material- und Geowissenschaften, Technische Universität Darmstadt, Petersenstr. 23, 64287 Darmstadt, Germany. E-mail: bekheet@materials.tu-darmstadt.de*

[b]*Technische Universität-Bergakademie Freiberg, Freiberg High Pressure Research Centre, Institut für Anorganische Chemie, Leipziger Straße 29, 09599 Freiberg, Germany*

† Electronic supplementary information (ESI) available: Experimental details; Raman spectra. See DOI: 10.1039/c3ra22998j

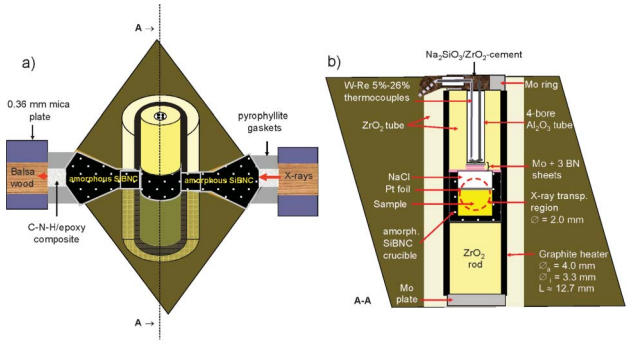

Fig. 2 Schematic cross sections of the multi-anvil octahedral pressure cell (b) and gasketing scheme (a) employed for this study. This synchrotron multi-anvil assembly comprises of only amorphous and low *Z*-materials along the beam path, thus providing high X-ray transmission and no additional reflections from the sample environment.[14]

Research Centre were employed (Fig. 2).[15] These assemblies have low X-ray absorption and don't show any additional reflections from the sample environment.

The initial c-In_2O_3 specimen doped with 7.5 at% Mn was synthesized by a hydrothermal method followed by calcination in air at 500 °C for 2 h (see Experimental part in the ESI†). Fig. 3 displays the X-ray powder diffraction pattern (XRPD) and Rietveld difference plot of the material. The structure refinement confirms a phase-pure solid solution c-$In_{1.85}Mn_{0.15}O_3$ with a slightly diminished lattice parameter (a = 10.0922(6) Å) compared to that of undoped c-In_2O_3 (a = 10.126(7) Å).[5] This decrease is due to the substitution of Mn^{3+} for In^{3+} [r (Mn^{3+}, high spin) = 65 pm, r (In^{3+}) = 79 pm; both ions are 6-fold coordinated].[16] No overstructure reflections can be seen and thus the substitution can be assumed to be close to random. Despite recent works pointing out the stabilization of Mn^{2+} in c-In_2O_3,[17] we did not observe Mn^{2+} ions in our specimens. The large ionic radius of Mn^{2+} ions (82 pm)[16] should result in an increase of the lattice parameters of indium oxide that was not observed in our experiments. Also recent UV-vis spectroscopy and magnetic characterization results confirm Mn^{3+} in c-In_2O_3 materials.[18,19]

The homogeneity of the specimen was further investigated by TEM inspection (Fig. 3b–d). As shown in Fig. 3b, the specimen consists of cube-shaped crystals with a typical intrinsic porosity. The latter is due to the synthesis conditions of our specimen, that was formed upon thermal decomposition of indium hydroxide accompanied by the escape of water molecules.[20] The energy dispersive X-ray spectroscopy (EDS, Fig. 3d) analysis on several single crystals confirms the incorporation of manganese into the c-In_2O_3.

Fig. 4 shows the energy-dispersive X-ray diffraction patterns of the c-$In_{1.85}Mn_{0.15}O_3$ specimen compressed to ~8 GPa and stepwise heated up to 950 °C. These *in situ* time-resolved data at given p–T conditions demonstrate some rather unexpected behaviour of the c-$In_{1.85}Mn_{0.15}O_3$ sample.

Compression of the c-$In_{1.85}Mn_{0.15}O_3$ specimen to 8 GPa at room temperature leads to a significant broadening of the XRD reflections due to deviatoric stress; the peak positions are shifted

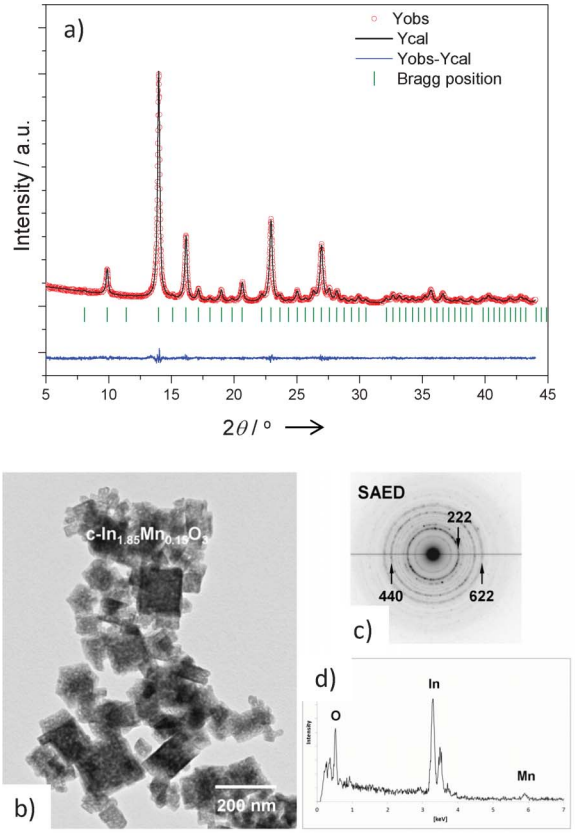

Fig. 3 (a) Structure refinement plot (*ex situ* powder XRD) of the initial bixbyite-type c-$In_{1.85}Mn_{0.15}O_3$ (*Ia*-3, No. 206, Z = 16, a = 10.0922(6) Å) showing observed (red circles) and calculated (black solid line) intensities. Tick marks refer to c-In_2O_3 structure (R_{Bragg} = 1.00). (b) TEM micrograph with the corresponding SAED pattern (c). The incorporation of manganese into c-In_2O_3 is verified by EDS (d).

to lower d-spacings with increasing pressure, consistent with the previous studies' observations on compressed undoped c-In_2O_3.[6,12] Subsequent heating of the specimen at this pressure leads to several consecutive effects: (i) upon heating the diffractions peaks become narrow because of the release of the internal stress, (ii) a series of new reflections appear at 700 °C; these reflections are attributed to orthorhombic indium oxyhydroxide (o-InOOH, $P2_1nm$, No. 31, Z = 2, a = 5.2642, b = 4.5667, and c = 3.2721 Å); the o-InOOH reflections disappeared again at 800 °C, (iii) at 950 °C only reflections of corundum-type rh-In_2O_3 are observed, (iv) the specimen rapidly quenched from 950 °C to room temperature shows only rh-In_2O_3 reflections. The structure refinement of this specimen recovered to the ambient pressure confirmed the rh-In_2O_3 ($R\bar{3}c$, No. 167, Z = 6, a = 5.482704(5) and c = 14.505157(2) Å) phase and indicated the presence of about 2 wt% cubic (rock salt type) MnO (Fm-3m, No. 225, a = 4.4464(5) Å) (Fig. 5a). As depicted in Fig. 5b–d, the phase separation was also detectable *via* TEM imaging. EDS revealed that the rh-In_2O_3 does not contain a detectable amount of Mn, but a small amount of a separate phase of pure MnO, which was also confirmed by EDS analysis, was found instead. Furthermore, a significant amount of turbostratic carbon was observed in the specimen; MnO particles were observed in the vicinity of carbon segregates. Elemental

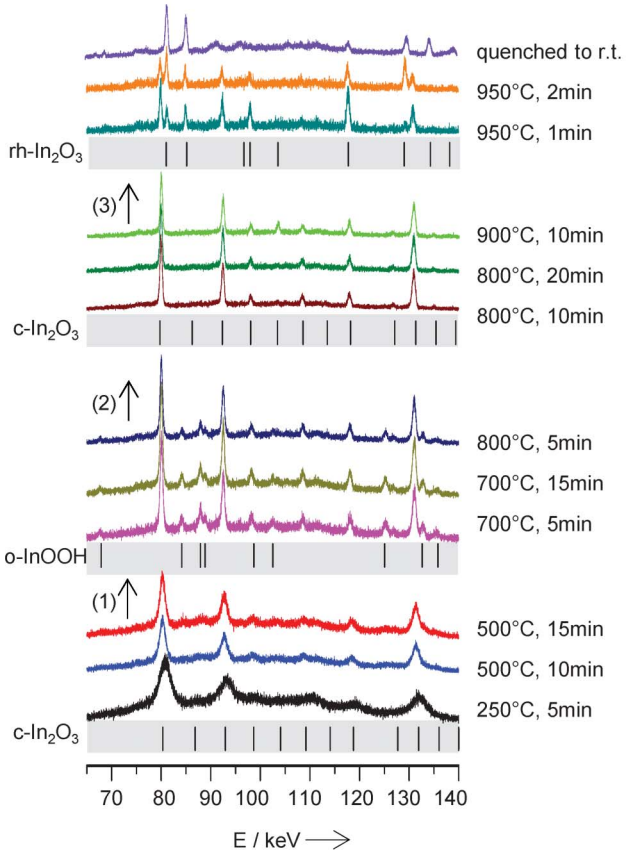

Fig. 4 Energy-dispersive XRD patterns obtained *in situ* in a multi-anvil assembly: c-$In_{1.85}Mn_{0.15}O_3$ specimen compressed at 8 GPa and step-wise heated up to 950 °C with different dwelling intervals. The tick marks refer to the calculated Bragg positions of c-In_2O_3, o-InOOH and rh-In_2O_3. Arrows indicate the intermediate occurrence (1) and disappearance (2) of an o-InOOH compound, and formation of corundum type rh-In_2O_3 (3).

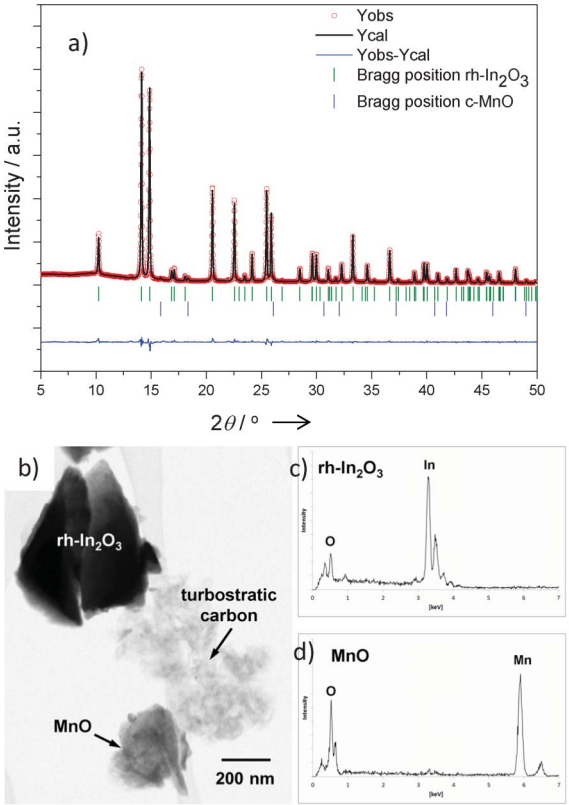

Fig. 5 (a) Structure refinement plot (*ex situ* powder XRD) of a c-$In_{1.85}Mn_{0.15}O_3$ specimen recovered after being compressed to 8 GPa and heated to 950 °C, showing observed (red circles) and calculated (black solid line) intensities. Complete phase segregation into pure rh-In_2O_3 ($R\bar{3}c$, No. 167, $Z = 6$, $a = 5.482704(5)$ and $c = 14.505157(2)$ Å) and rocksalt-type c-MnO ($a = 4.4464(5)$ Å, fraction 2.14%) is discernible. Refinement residuals were $R_{Bragg} = 2.32$ for rh-In_2O_3 and $R_{Bragg} = 2.64$ for c-MnO. (b) TEM and EDS characterization (c, d) confirm undoped rh-In_2O_3 and c-MnO and indicate the formation of the turbostratic carbon.

carbon (graphite) as well as carbonates and acetates were not observed in the initial c-$In_{1.85}Mn_{0.15}O_3$ specimen as confirmed by elemental analysis, Raman and FTIR spectroscopy. The Raman spectra (see ESI†) confirm turbostratic carbon in the amorphous SiBCN crucibles (used in the multi-anvil assembly) and the recovered specimens, as well.

The decomposition of Mn-doped c-In_2O_3 into undoped rh-In_2O_3 and MnO is surprising. As the rh-In_2O_3 polymorph is metastable over the complete enthalpy–pressure diagram,[5] the expected sequence of phase transitions with increasing pressure is c-In_2O_3 → o′-In_2O_3 → o″-In_2O_3. In another experiment, we observed that an undoped c-In_2O_3 specimen transforms under similar conditions (8.5 GPa/850 °C) into o′-In_2O_3. The metastable rh-In_2O_3 polymorph appears upon decompression of o′-In_2O_3.[21] In the present study rh-In_2O_3 crystallizes upon decomposition of Mn-doped c-In_2O_3 at high pressure and temperature.

The formation of MnO in the recovered specimen may be explained as follows. Mn-doped c-In_2O_3 decomposes into undoped rh-In_2O_3 and Mn_2O_3. According to a recently published p–T diagram,[9] under the p–T conditions of our experiment Mn_2O_3 melts and irreversibly reduces to Mn_3O_4. The further reduction of Mn_3O_4 to MnO is achieved by carbon.[22] The reducing conditions occurring during the synthesis stabilize MnO against reoxidation. At ambient oxygen pressure, MnO becomes stable only at $T >$ 1850 K (1577 °C) which is a significantly higher temperature than that applied in our synthesis (950 °C).[23] At this temperature MnO becomes stable if $p(O_2) < 10^{-7}$ bar. It is worth noting that the recent high-pressure experiments demonstrated also the decomposition and reduction of manganese oxides.[9,24]

Rutile-type indium oxyhydroxide (oxide-hydroxide) o-InOOH appears as a transient intermediate at 8 GPa and at 700–800 °C. o-InOOH is usually synthesized from c-$In(OH)_3$ under solvothermal conditions/dry pressure routes at 0.1–4 GPa and 350–600 °C.[25] The observation of o-InOOH in the present study points out the reaction between c-In_2O_3 and H_2O under high-pressure and high-temperature conditions. The possible sources of water can be either the pressure standard (NaCl) or the specimen itself. It is worthy of note that o-InOOH was also observed as a side phase in a recent synthesis of $InMnO_3$ and In–Mn–Fe–O perovskites as well as corundum-type $In_{2-2x}Zn_xSn_xO_3$ oxides performed at 6 GPa/1100–1500 °C and 7 GPa/1000 °C, respectively.[26–28] Hence, the appearance of o-InOOH under high-pressure high-temperature

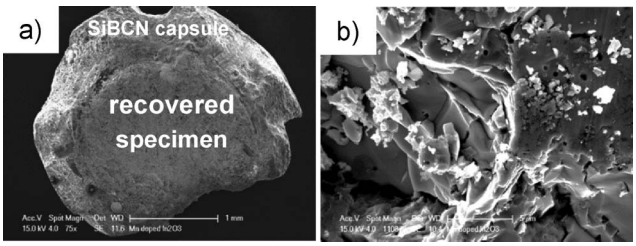

Fig. 6 Scanning electron micrographs of the specimens recovered from the *in situ* multi-anvil in SiBCN capsule (a) and high magnification images of recovered specimen (b).

conditions in indium-containing specimens can be an issue for the synthesis of binary and ternary indium oxides and requires further, more careful, study.

The scanning electron micrographs (Fig. 6) visualize the amount of the specimen recovered from the *in situ* multi-anvil experiment. Fig. 6 a shows a cross-section of the SiBCN-crucible with the recovered specimen. The apparent porosity in Fig. 6 b may indicate water evaporation from the cell which in turn may go along with crystallization of o-InOOH and/or carbon oxides released during the MnO formation.

In summary, our *in situ* time-resolved characterization of Mn-doped bixbyite-type c-In_2O_3 at 8 GPa indicates two effects: (i) the appearance of indium oxyhydroxide (InOOH) as a transient intermediate at 700–800 °C and (ii) decomposition of the initial material into undoped corundum-type rh-In_2O_3 and MnO at 950 °C. The reduction of Mn^{3+} (in c-In_2O_3) to Mn^{2+} (in Mn_3O_4 and MnO) is explained by the interplay of two processes, *i.e.* the thermodynamic stability of Mn_3O_4 under particular *p–T* conditions and the reaction of Mn_3O_4 with carbon from the SiBCN crucible.

Acknowledgements

The financial support by the German Research Foundation DFG within the priority programme SPP1236 (Synthesis, *in situ* characterization and quantum mechanical modelling of Earth Materials, oxides, carbides and nitrides at extremely high pressures and temperatures) and DESY are greatly acknowledged. The authors would also like to thank Christian Lathe for technical support and the Helmholtz Centre Potsdam, GFZ German Research Centre for Geosciences, for the opportunity to perform measurements at the MAX200X press.

Notes and references

1 A. Walsh, J. L. F. Da Silva and S. H. Wei, *J. Phys.: Condens. Matter*, 2011, **23**, 334210.
2 E. Guilmeau, D. Berardan, C. Simon, A. Maignan, B. Raveau, D. O. Ovono and F. Delorme, *J. Appl. Phys.*, 2009, **106**, 053715.
3 A. Gurlo, *Nanoscale*, 2011, **3**, 154–165.
4 A. A. Belik, T. Furubayashi, Y. Matsushita, M. Tanaka, S. Hishita and E. Takayama-Muromachi, *Angew. Chem., Int. Ed.*, 2009, **48**, 6117–6120.
5 A. Gurlo, P. Kroll and R. Riedel, *Chem.–Eur. J.*, 2008, **14**, 3306–3310.
6 H. Yusa, T. Tsuchiya, N. Sata and Y. Ohishi, *Phys Rev B*, 2008, 77.
7 A. Gurlo, D. Dzivenko, P. Kroll and R. Riedel, *Phys. Status Solidi RRL*, 2008, **2**, 269–271.
8 J. Santillan, S. H. Shim, G. Y. Shen and V. B. Prakapenka, *Geophys. Res. Lett.*, 2006, **33**, L15307.
9 S. V. Ovsyannikov, A. M. Abakumov, A. A. Tsirlin, W. Schnelle, R. Egoavil, J. Verbeeck, G. Van Tendeloo, K. V. Glazyrin, M. Hanfland and L. Dubrovinsky, *Angew. Chem., Int. Ed.*, 2013, **52**, 1494–1498.
10 D. Liu, W. W. Lei, B. Zou, S. D. Yu, J. Hao, K. Wang, B. B. Liu, Q. L. Cui and G. T. Zou, *J. Appl. Phys.*, 2008, **104**, 083506.
11 J. Qi, J. F. Liu, Y. He, W. Chen and C. Wang, *J. Appl. Phys.*, 2011, **109**, 063520.
12 H. Yusa, T. Tsuchiya, J. Tsuchiya, N. Sata and Y. Ohishi, *Phys Rev B*, 2008, 78.
13 T. Irifune, *Mineral. Mag.*, 2002, **66**, 769–790.
14 M. R. Schwarz, C. Schimpf and T. Barsukova, unpublished work.
15 M. Schwarz, T. Barsukova, C. Schimpf, D. Šimek, C. Lathe, D. Rafaja and E. Kroke, in *HASYLAB Users' Meeting*, Hamburg, Germany, 2010.
16 R. D. Shannon and C. T. Prewitt, *Acta Crystallogr., Sect. B: Struct. Crystallogr. Cryst. Chem.*, 1969, **25**, 925–946.
17 Y. K. An, D. Q. Feng, L. S. Duan, Z. H. Wu and J. W. Liu, *J Phys D Appl Phys*, 2012, 45.
18 G. Peleckis, X. L. Wang and S. X. Dou, *J. Magn. Magn. Mater.*, 2006, **301**, 308–311.
19 S. S. Farvid, N. Dave, T. Wang and P. V. Radovanovic, *J. Phys. Chem. C*, 2009, **113**, 15928–15933.
20 G. Miehe, S. Lauterbach, H.-J. Kleebe and A. Gurlo, *J. Solid State Chem.*, 2013, **198**, 364–370.
21 M. F. Bekheet, M. R. Schwarz, S. Lauterbach, H.-J. Kleebe, P. Kroll, R. Riedel and A. Gurlo, *Angew. Chem., Int. Ed.*, 2013, DOI: 10.1002/anie.201300644.
22 G. J. W. Kor, *Metall. Trans. B*, 1978, **9**, 307–311.
23 R. K. Amankwah and C. A. Pickles, *J. Therm. Anal. Calorim.*, 2009, **98**, 849–853.
24 H. Serier-Brault and M. Jansen, *Solid State Sci.*, 2011, **13**, 326–330.
25 A. Sano, T. Yagi, T. Okada, H. Gotou, E. Ohtani, J. Tsuchiya and T. Kikegawa, *J. Mineral. Petrol. Sci.*, 2008, **103**, 152–155.
26 D. A. Rusakov, A. A. Belik, S. Kamba, M. Savinov, D. Nuzhnyy, T. Kolodiazhnyi, K. Yamaura, E. Takayama-Muromachi, F. Borodavka and J. Kroupa, *Inorg. Chem.*, 2011, **50**, 3559–3566.
27 A. A. Belik, T. Furubayashi, H. Yusa and E. Takayama-Muromachi, *J. Am. Chem. Soc.*, 2011, **133**, 9405–9412.
28 C. A. Hoel, J. M. G. Amores, E. Moran, M. A. Alario-Franco, J. F. Gaillard and K. R. Poeppelmeier, *J. Am. Chem. Soc.*, 2010, **132**, 16479–16487.

